Journal of Materials Science

Lightweight and highly conductive silver nanoparticles functionalized meta-aramid nonwoven fabric for enhanced electromagnetic interference shielding

--Manuscript Draft--

Manuscript Number:	JMSC-D-20-06871R2
Full Title:	Lightweight and highly conductive silver nanoparticles functionalized meta-aramid nonwoven fabric for enhanced electromagnetic interference shielding
Article Type:	Manuscript (Regular Article)
Keywords:	Meta-aramid nonwoven fabric; Silver nanoparticles; Electrical conductivity; electromagnetic interference shielding
Corresponding Author:	Liang Jiang Qingdao University Qingdao, -- Please Select -- CHINA
Corresponding Author Secondary Information:	
Corresponding Author's Institution:	Qingdao University
Corresponding Author's Secondary Institution:	
First Author:	Yanfen Zhou
First Author Secondary Information:	
Order of Authors:	Yanfen Zhou
	Wenyue Li
	Lele Li
	Zhenhua Sun
	Liang Jiang
	Jianwei Ma
	Shaojuan Chen
	Xin Ning
	Fenglei Zhou
Order of Authors Secondary Information:	
Abstract:	High performance electromagnetic interference (EMI) shielding material that that can function properly under extreme working conditions is critical for their practical applications. Herein, flexible and highly conductive meta -aramid (PMIA) nonwoven fabrics were fabricated by combining polydopamine (PDA) modification and electroless silver plating. The PDA modification greatly enhanced the efficient deposition of silver nanoparticles (AgNPs) and the interfacial cohesion between the AgNPs and the PMIA fibers. The silver-coated PMIA non-woven fabric exhibited an electrical conductivity as high as 0.29 Ω/sq, an excellent EMI shielding effectiveness (SE) of 92.6 dB and a high absolute EMI SE of 8194.7 dB·cm 2 ·g -1 . In addition, the silver-coated PMIA non-woven fabric maintained high electrical conductivity and EMI SE after being subjected to washing, bending and torsion deformations, high/low temperature, strong acidic/alkaline solutions and different organic solvents. These results have clearly demonstrated that PMIA nonwoven fabric can be made highly electrically conductive by using a simple and highly scalable method. It holds great promise for the applications in EMI shielding materials that can be used in various harsh conditions.
Funding Information:	the Shandong “Taishan Youth Scholar Program” (tsqn201909100) — Dr Yanfen Zhou

	Shandong Provincial Key Research and Development Program, China (2019GGX102071)	Dr Yanfen Zhou
	National Natural Science Foundation of China (51703108)	Dr. Liang Jiang

Cover Letter

Dear editor,

Thank you very much for all you support in processing our manuscript entitled "Lightweight and highly conductive silver nanoparticles functionalized meta-aramid nonwoven fabric for enhanced electromagnetic interference shielding" (Manuscript number: JMSC-D-20-06871). We have revised the manuscript according to the reviewer's comments. The detailed responses to the reviewer's comments are attached in a separate "Response to Reviewer Comments" file.

We look forward to hearing from you regarding our submission. We would be glad to respond to any further questions and comments that you may have.

Thank you and best regards.

Yours sincerely,

Liang Jiang (Email: liang.jiang@qdu.edu.cn)

Responses to Reviewer

The authors greatly appreciate the reviewer's very useful and constructive comments and suggestions and have revised the manuscript accordingly. The detailed responses to the reviewer are listed as follows:

Reviewer #1: The manuscript entitled "Lightweight and highly conductive silver nanoparticles functionalized meta-aramid nonwoven fabric for enhanced electromagnetic interference shielding" The results of this manuscript are interesting, such as high electric conductivity, and EMI shielding properties of the PMIA/PDA/Ag composite fabric. But there are still some shortcomings in this paper that need to be further modified."

1. When the $AgNO_3$ concentration is 8g/L, the value of EMI SE is 5.54dB. When the AgNO3 concentration is increased to 10g/L, the EMI SE value reaches 92.68dB. However, it can be seen from the SEM image of PMIA/PDA/Ag-8 that a lot of Ag nanoparticles are deposited on PMIA fibers, which can also form a complete conductive network. But the dB value is lower than 10, the author should repeat the experiment to verify.

Response to 1: We thank the reviewer for pointing this out. The EMI shielding performance of the silver-coated PMIA nonwoven fabric prepared with $AgNO_3$ concentration of 8 g/L (PMIA/PDA/Ag-8) was measured again and an average EMI SE of 5.97 dB over the frequency of 8.2-12.4 Hz was obtained. In fact, when the $AgNO_3$ concentration was 8 g/L, the sheet resistance of silver-coated PMIA nonwoven fabric was 24.58 Ω/sq, which is much higher than that of the silver-coated PMIA nonwoven fabric prepared with $AgNO_3$ concentration of 10 g/L (0.29 Ω/sq). This indicates that the conductive network for PMIA/PDA/Ag-8 was not as complete as that of PMIA/PDA/Ag-10.

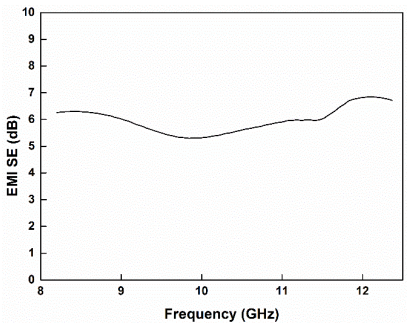

Figure R1. The EMI SE of PMIA/PDA/Ag-8

2. How identify the density of the samples? The authors should give the calculation methods.

Response to 2: The authors thank the reviewer for this suggestion. The area density of silver-coated PMIA was determined based on the content of PDA and AgNPs in PMIA nonwoven fabric from TG test. This information has been added in the manuscript and highlighted in yellow on page 15.

3. The microporous structure of PMIA will affect the shielding of electromagnetic waves. In the introduction, the effect of sample morphology and microporous structure on electromagnetic shielding should be added.

Response to 3: We thank the reviewer for pointing this out. The effect of sample morphology and microporous structure on electromagnetic shielding has been added in the introduction and highlighted in yellow.

4. PMIA/PDA/Ag composite fabrics are used in a variety of complex environments, the rubbing fastness of Ag nanoparticles and PMIA is very important. The author should add this test.

Response to 4: We thank the reviewer for this good suggestion. Actually, we did the abrasion test of PMIA/PDA/Ag-10 nonwoven fabric by using a Martindale fabric abrasion tester (Model: YG 401-H), and found that the sheet resistance increased by 10.97% after 100 abrasion cycles, showing decent coating durability. However, because the PMIA nonwoven fabric is a kind of spun-laced nonwoven fabric which has a poor abrasion resistance itself, fabric surface fuzzing and pilling of short PMIA fibers occurred rapidly and even some PMIA fibers fell off during the abrasion test before AgNPs peeled off from its surface (as can be seen from Figure R2), which made it tricky to effectively evaluate the rubbing fastness of AgNPs on PMIA fibers. Therefore, we did not put this result in the manuscript. A feasible solution to improve the abrasion resistance of the silver-coated PMIA nonwoven fabric could be to introduce another polymer as the protective layer, such as PDMS, TPU, PFDT, SEBS, PPy and so on as reported in the literature (ACS Appl. Mater. Interfaces 2019, 11, 10883-10894; Carbon 144 (2019) 101-108; Chemical Engineering Journal 364 (2019) 493-502; ACS Appl. Mater. Interfaces 2019, 11, 34338-34347; Adv. Funct. Mater. 2019, 29, 1806819). Those polymer coating layers could also help to protect the silver coating layer from oxidation. We are currently working on this and hope to contribute to this part of work

soon.

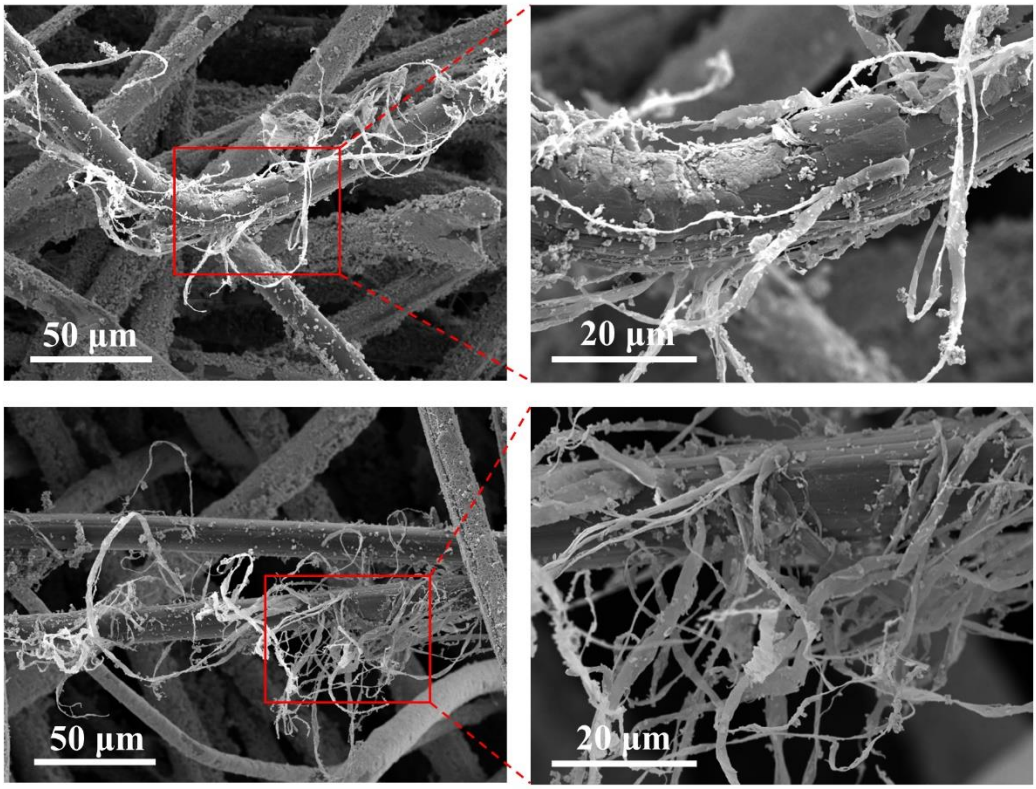

Figure R2. SEM image of the PMIA/PDA/Ag-10 nonwoven fabric after 100 abrasion cycles

5. For the silver-coated PMIA nonwoven fabric, although its SEA value is greater than SER. But its shielding mechanism is mainly reflection, the author should further explain the reason. You can refer to the literature to further explain.

[1] Tan Y-J, Li J, Gao Y, Li J, Guo S, Wang M. A facile approach to fabricating silver-coated cotton fiber non-woven fabrics for ultrahigh electromagnetic interference shielding. Applied Surface Science. 2018;458: 236-44.

[2] Li T-T, Wang Y, Peng H-K, Zhang X, Shiu B-C, Lin J-H, Lou C-W. Lightweight, flexible and superhydrophobic composite nanofiber films inspired by nacre for highly electromagnetic interference shielding. Composites Part a-Applied Science and Manufacturing. 2020;128.

Response to 5: We thank the reviewer for this good suggestion and the related references. The explanation of the shielding mechanism has been improved and the corresponding references have been cited.

Lightweight and highly conductive silver nanoparticles functionalized *meta*-aramid nonwoven fabric for enhanced electromagnetic interference shielding

Yanfen Zhou [a], Wenyue Li [a], Lele Li [a], Zhenhua Sun [a], Liang Jiang [a,*], Jianwei Ma [a], Shaojuan Chen [b], Xin Ning [a], Fenglei Zhou [a, c]

[a] Industrial Research Institute of Nonwovens and Technical Textiles, College of Textiles and Clothing, Qingdao University, Qingdao, 266071, P. R. China

[b] Eco-Textile Collaborative Innovation Center, College of Textiles and Clothing, Qingdao University, Qingdao, 266071, P. R. China

[c] Centre for Medical Image Computing, University College London, London, WC1V 6LJ, UK

* Corresponding author: liang.jiang@qdu.edu.cn (Liang Jiang)

Abstract: High performance electromagnetic interference (EMI) shielding material that that can function properly under extreme working conditions is critical for their practical applications. Herein, flexible and highly conductive *meta*-aramid (PMIA) nonwoven fabrics were fabricated by combining polydopamine (PDA) modification and electroless silver plating. The PDA modification greatly enhanced the efficient deposition of silver nanoparticles (AgNPs) and the interfacial cohesion between the AgNPs and the PMIA fibers. The silver-coated PMIA non-woven fabric exhibited an electrical conductivity as high as 0.29 Ω/sq, an excellent EMI shielding effectiveness (SE) of 92.6 dB and a high absolute EMI SE of 8194.7 $dB \cdot cm^2 \cdot g^{-1}$. In addition, the silver-coated PMIA non-woven fabric maintained high electrical conductivity and EMI SE after being subjected to washing, bending and torsion deformations, high/low temperature, strong acidic/alkaline solutions and different organic solvents. These results have clearly demonstrated that PMIA nonwoven fabric can be made highly electrically conductive by using a simple and highly scalable method. It holds great promise for the applications in EMI shielding materials that can be used in various harsh conditions.

KEYWORDS: *meta*-aramid nonwoven fabric; silver nanoparticles; electrical conductivity; electromagnetic interference shielding

1. Introduction

With the widespread use of various mobile communications and electronic devices, electromagnetic pollution has attracted increasing attention [1]. There has been an increasing interest in developing functional materials that can effectively shield the electromagnetic radiation [2-6]. Metals and metal alloys have mostly been employed as electromagnetic interference (EMI) shielding materials owing to their excellent electrical conductivity [7]. However, the intrinsic heavy weight, limited physical flexibility and corrosion of metals seriously restricted their practical applications in aircraft, aerospace, automobiles and next-generation flexible electronics. Therefore, there is a large demand for the development of

lightweight and highly flexible functional materials with high EMI shielding effectiveness (SE). Conductive polymer composites consisting of polymer matrices and electrical conductive components are ideal candidates for EMI shielding materials due to their light weight and flexibility [8, 9]. Various conductive components including metal nanoparticles/nanowires [10-14], carbon nanotubes (CNTs)/nanofibers [15-17], graphene [18-20], transition metal carbide and/or nitride [21, 22] and their hybrids [23, 24] have been used as effective fillers to fabricate conductive polymer composites. Among them, silver has the highest conductivity (1.65×10^{-8} Ω·m of resistivity) and hence has been widely used in constructing EMI shielding polymer composites [12, 25]. Conductive polymer composites were generally fabricated by using two methods: one was directly incorporating the conductive fillers into polymer matrix [26-28] and the other one was depositing conductive components on the surface of polymeric substrates [29-31].

For polymer composites based EMI shieling materials, a desirable EMI SE was often achieved via high loading of conductive fillers or large coating thickness, which unavoidably caused an increase in the weight of resultant polymer composites. Previous studies have shown that the morphology of the conductive polymer composites has great influence on the EMI shielding effectiveness. For example, the formation of segregated structures helps to improve the electrical conductivity and EMI SE of conductive polymer composites because the conductive fillers form denser conductive paths around polymer regions instead of random dispersion in the entire polymer matrix [32, 33]. In addition, porous structures also help to reduce the density and improve the EMI SE of conductive polymer composites because the micrometer-sized pores provide large interfaces between air and the composite cell walls, which promotes multiple reflections in the composites and hence result in improved EMI shielding ability [34, 35].

More recently, nonwoven fabrics formed of randomly oriented polymeric fibers have emerged

as promising substrates for constructing EMI shielding materials because of their light weight and excellent flexibility [10, 36]. In addition, the porous structure of nonwoven fabrics helps to improve the EMI shielding ability through repeatedly reflection of electromagnetic waves. For example, Gao et al. [10] prepared highly conductive silver nanoparticle coated polypropylene nonwoven fabric with the average EMI SE of 48.2 dB in the frequency range of 8.2-12.4 GHz, Tan et al. fabricated silver-coated cotton fibers non-woven fabrics with the EMI SE as high as 71 dB [36]. Though high EMI SE values were achieved in ambient environment, the performance of those silver nanoparticle coated PP or cotton fiber nonwovens could be significantly deteriorated when exposed to extreme temperature and/or harsh corrosive chemicals. Therefore, the application of these materials in harsh conditions, such as high/low temperature or corrosive conditions is severely limited.

Polymetaphenylene isophthamide (PMIA), which is prepared by polycondensation of isophthalic chloride (ICI) and m-phenylenediamine (MPD), has excellent thermal stability, high mechanical strength, flame retardancy and corrosion resistance [37, 38]. PMIA nonwoven fabrics are considered to be an promising substrate material for applications under extreme conditions. However, to date there has been little investigation of PMIA nonwovens as EMI shielding materials.

To develop EMI shielding materials integrating light weight, high flexibility, outstanding electrical conductivity, reliable thermal and chemical stability, in the present study, commercially available PMIA nonwoven fabric was explored as a substrate to prepare first-of-its kind EMI shielding materials by combining bio-inspired polydopamine modification and highly scalable electroless silver plating. The effect of polydopamine modification on the deposition of silver nanoparticles (AgNPs) on PMIA nonwoven fabric was firstly investigated. Then, the bonding fastness of silver coating on the surface of PMIA non-woven fabric was determined. The focus was on the evaluation of electrical conductivity and electromagnetic

shielding performance of silver coated PMIA non-woven fabric under various conditions such as washing, mechanical bending, exposing to wide range of temperature (-80 to 200 °C), acid/alkali solutions and several organic solvents.

2. Experimental

2.1 Materials

The *meta*-aramid non-woven fabric with an area density of 50 $g \cdot m^{-2}$ and a thickness of 0.3 mm (the average diameter of a single fiber is 13.5 μm) was supplied by Jiangsu Kaidun New Material Co., Ltd, China. The non-woven fabric was prepared by web-forming and spun-lacing of *meta*-aramid staple fibers. Dopamine hydrochloride (DA·HCl) was purchased from Macklin Biochemical Co., Ltd, China. Trimethylol aminomethane (Tris) was purchased from Beijing Solarbio Science and Technology Co., Ltd, China. Silver nitrate ($AgNO_3$), glucose, sodium hydroxide (NaOH), ethanol and ammonia ($NH_3 \cdot H_2O$) were purchased from Sinopharm Chemical Reagent Co., Ltd, China.

2.2 Dopamine polymerization on PMIA non-woven fabric surface

First of all, dopamine solution with a concentration of 2 g/L was prepared by dissolving a certain amount of DA·HCl in deionized water, pH of the solution was adjusted to 8.5 by adding Tris. Then, the PMIA non-woven fabric was immersed in the above dopamine aqueous solution for 24 h at room temperature. Finally, the PMIA non-woven fabric was separated and rinsed thoroughly with deionized water and dried in vacuum oven at 60 °C overnight. The obtained sample was denoted as PMIA/PDA.

2.3 Electroless deposition of silver nanoparticles on PMIA/PDA surface

Firstly, a silver-plating bath was prepared as follows: a certain amount of silver nitrate was dissolved in deionized water to form silver nitrate solution with the concentration ranging from 4 to 12 g/L, the ammonia solution with a volume fraction of 2% was added dropwise to the silver nitrate solution under vigorous magnetic stirring until the solution became transparent.

pH of the above solution was adjusted to 11 by using NaOH solution and then ammonia solution was added dropwise to the ammoniacal silver nitrate solution until the solution became transparent again. The PMIA/PDA nonwoven fabrics were immersed into the solution and activated for 30 min. Then, glucose solution as a reducing agent was added dropwise to the silver-plating bath. The reaction was allowed to proceed under magnetic stirring at 30 °C for 1 h. Finally, the silver-plated PMIA non-woven fabric was separated, rinsed with deionized water three times and dried in vacuum at 60 °C for 24 h. The silver-plated PMIA nonwovens obtained at $AgNO_3$ concentration of 4 g/L, 6 g/L, 8 g/L, 10 g/L and 12 g/L were referred as PMIA/PDA/Ag-4, PMIA/PDA/Ag-6, PMIA/PDA/Ag-8 PMIA/PDA/Ag-10 and PMIA/PDA/Ag-12 respectively. The overall preparation process of electrically conductive PMIA nonwoven fabric is illustrated schematically in Figure 1.

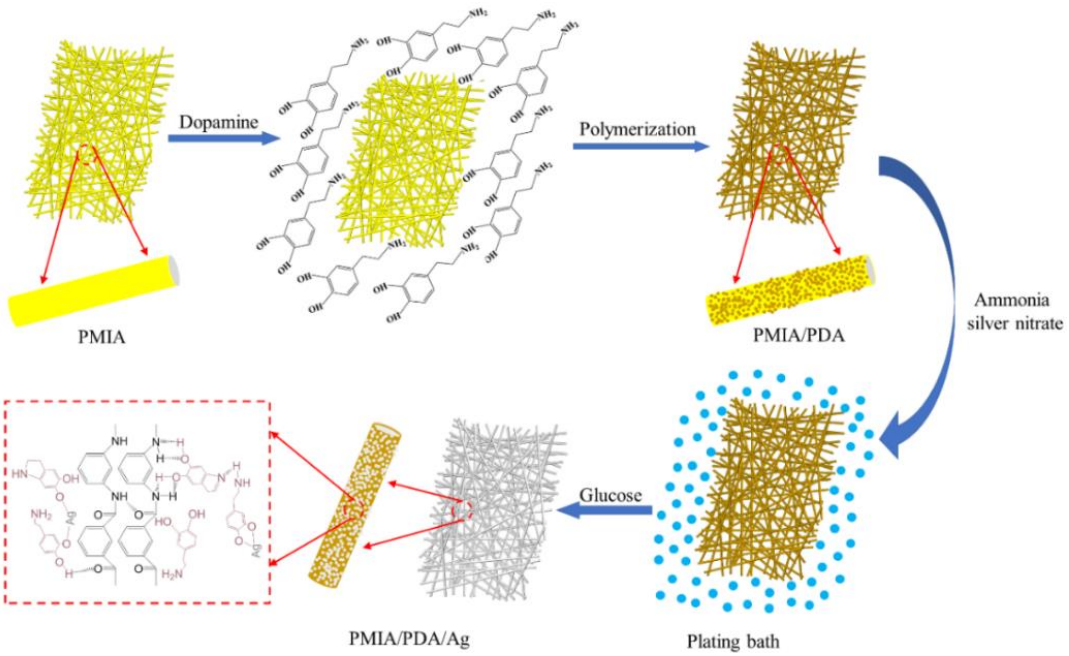

Figure 1. Schematic illustration of the procedure for preparing silver-coated PMIA non-woven fabric.

2.4 Characterization

Surface morphology of PMIA non-woven fabrics was observed by using scanning electron microscopy (SEM) (VEGA3, TESCAN, Czech). The samples were sputter-coated with a thin

layer of gold prior to observation and SEM images with various magnifications were taken at a voltage of 10 kV.

The surface chemical composition of PMIA non-woven fabric was measured by using an X-ray photoelectron spectroscopy (XPS) (ESCALAB 250XI, Thermo Fisher Scientific, USA) with an Al Kα X-ray source (1486.6 eV photons). The X-ray source was run at a reduced power of 150 W. The pressure in the analysis chamber was maintained at 10^{-8} Torr during each measurement. All binding energies (BEs) were referenced to the C1s hydrocarbon peak.

The formation of PDA on the surface of PMIA non-woven fabric was characterized by using fourier transform infrared spectroscopy (FTIR) (NICOLET iS10, Thermo Fisher Scientific, USA). The tests were conducted in ATR mode and the spectrum was collected at a resolution of 16 cm^{-1} and a wavelength range of 4000 – 675 cm^{-1}.

The X-ray diffraction pattern of the samples was obtained by exploiting an X-ray diffractometer (XRD, Rigaku Ultima IV, Japan) using Cu Kα radiation with a wavelength of 1.54056 Å. The measurements were conducted in a reflection mode at the 2θ range of 5 – 90° with a scanning speed of 5°/min.

Thermal stability and the weight percentage of Ag nanoparticles of the PMIA composite nonwoven fabrics were measured by exploiting a TG/DSC synchronous thermal analyzer (STA 449 F3, NETZSCH GmbH, Germany). The samples were dried in vacuum at 60 °C for 24 hours before testing. The thermal decomposition curves were recorded in the temperature range of 40 - 800 °C with a heating rate of 20 °C /min in an N_2 atmosphere.

The water contact angle test was conducted by using an automatic contact angle measuring instrument (XG-CAMD3, Shanghai Xuanyichuangxi Industrial Equipment Co., Ltd. China).

The electrical sheet resistance of silver-coated PMIA non-woven fabric was measured according to GB/T 1552-1995 by using a four-probe tester (ST-2258C, Suzhou Jingge Electronic Co., Ltd, China). The measurements were taken at five different locations and the

average electrical resistance was used.

The electrical resistance changes upon bending and torsion deformations of the nonwovens were recorded using a precision source/measure unit (B2901A, Keysight, USA).

The EMI shielding performance of the silver-coated PMIA non-woven fabric was investigated by using an ENA network analyzer (ZNB 20, Rohde & Schwarz, Germany) in the frequency range of 8.2 – 12.4 GHz (X band) by means of waveguide method at room temperature [39]. The nonwoven fabrics were cut into rectangle plates with a dimension of 22.9 mm × 10.2 mm for measurement.

The tensile test of the PMIA nonwoven fabric was carried out according to GB/T 24218.3-2010 by using an universal testing machine (Model 5956, Instron Instruments, USA) with a loading rate of 100 mm/min and a gauge length of 20 mm. Five specimens were tested to for each material and the average value of tensile strength and elongation at break was used.

3. Results and Discussions

3.1 Surface PDA modification of PMIA non-woven fabric

It is widely known that dopamine is easily oxidized by dissolved oxygen in an aqueous solution, which then initiates a self-polymerization-crosslinking reaction to form a tightly adhered layer on almost all types of organic/inorganic surfaces [40, 41]. When the PMIA nonwoven fabric was put into a freshly prepared dopamine aqueous solution and soaked for a period of time, surface modified PMIA nonwoven fabric with a polydopamine layer attached to the surface would be obtained. It can be seen from the upper image in Figure 2a that the pristine PMIA nonwoven fabric appeared to be white and PMIA fibers had smooth surface (Figure 2b). After dopamine modification, the PMIA nonwoven fabric turned dark brown (the lower image in Figure 2a) and the surface of the PMIA fibers became coarse (Figure 2c) due to the formation of polydopamine.

The presence of polydopamine on the surface of PMIA fibers were confirmed by XPS

measurement. Figure 2d - i shows the XPS wide-scan spectra, C 1s and N 1s core-level spectra of pristine PMIA (Figure 2d - f) and PDA modified PMIA (Figure 2g - i) nonwoven fabrics. It can be seen from Figure 2d and 2g that the wide-scan spectrum of both PMIA and PMIA/PDA sample comprised three distinct peaks at about 285 eV, 400 eV and 532 eV corresponding to C 1s, N 1s and O 1s, respectively. Figure 2e shows that the C 1s core-level spectrum of pristine PMIA could be curve-fitted with three peaks with binding energies of 284.4 eV for -C-C- species, 285.5 eV for -C-N- species and 287.8 eV for -C=O- species respectively. An additional fitted peak at 286.1 eV ascribed to the -C-O- species appeared in the C 1s peak of PMIA/PDA (Figure 2h). Moreover, compared with pristine PMIA nonwoven fabric, the N 1s core-level spectrum of PMIA/PDA (Figure 2i) had a new peak with the binding energy of 398.5 eV for -N=, which was associated with the indole group during dopamine self-polymerization [42]. These results confirmed that polydopamine was successfully deposited on the surface of PMIA fibers. The presence of characteristic peaks at 1569 cm^{-1} and 1350 cm^{-1}, which belonged to the vibration of aromatic ring and indole group in dopamine, in the FTIR spectrum of PMIA/PDA (Figure S1, Supporting Information) also indicated the presence of PDA layer on the PMIA nonwoven fabric. The interaction between PDA and PMIA substrate is probably intermolecular force due to the insert surfaces of PMIA fibers [43].

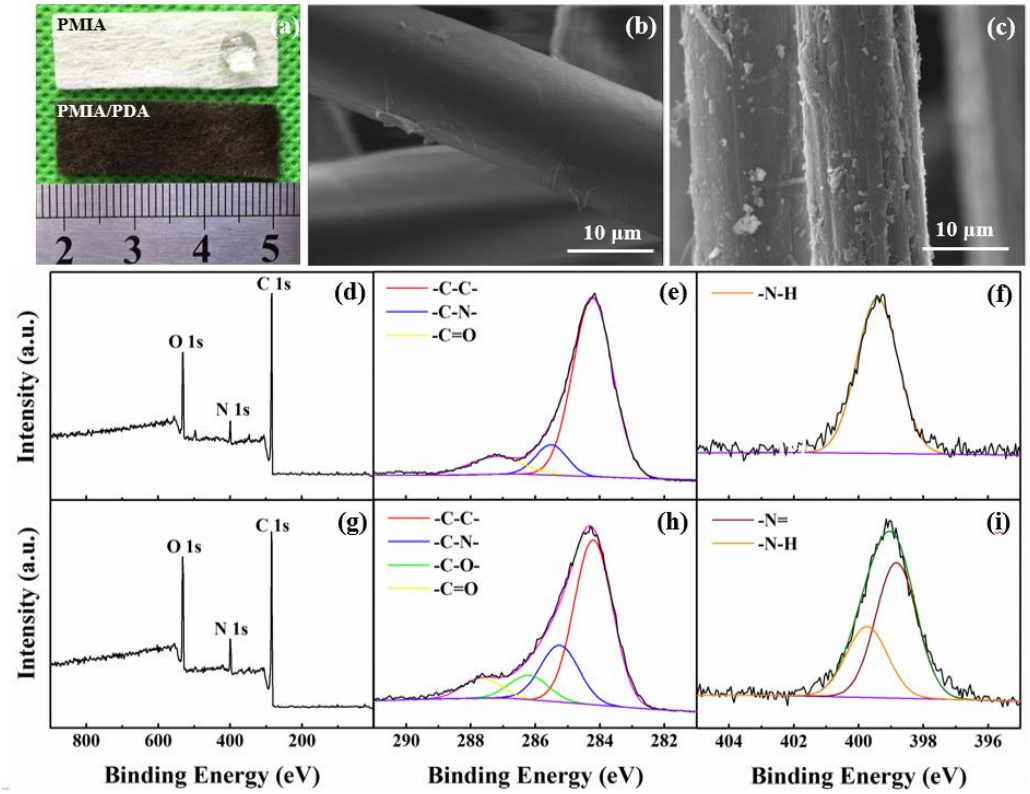

Figure 2. The optical picture of pristine PMIA and PMIA/PDA nonwoven fabric (a); SEM image of pristine PMIA nonwoven fabric (b) and PMIA/PDA nonwoven fabric (c); XPS wide-scan spectra (d), C 1s peaks (e) and N 1s peaks (f) of pristine PMIA non-woven fabric; XPS wide-scan spectra (g), C 1s peaks (h) and N 1s peaks (i) of PMIA/PDA nonwoven fabric.

The water contact angle of pristine PMIA nonwoven fabric was 132° (Figure S2, Supporting Information), indicating its hydrophilicity, but in contrast, the water droplet spread immediately on the surface of PMIA/PDA nonwoven fabric (Movie 1, Supporting Information). This dramatic change in surface hydrophilicity of PMIA nonwoven fabric after polydopamine modification was expected to greatly favor the efficient absorption of silver ions and hence increase the amount of silver nanoparticles deposited on the PMIA nonwoven fabric.

3.2 Silver nanoparticles functionalized PMIA non-woven fabric

After electroless silver plating, the PMIA nonwoven fabric appeared to silver color but retained good flexibility as shown in Figure 3a. Continuous silver coating was observed clearly on the surface of PMIA fibers (Figure 3b). The strong peaks for Ag in the XPS wide-scan shown in

Figure 3c confirmed the successful deposition of silver nanoparticles on the PMIA fiber surface. The two peaks at 367.5 eV and 373.5 eV corresponding to Ag $3d_{5/2}$ and Ag $3d_{3/2}$ were contributed to the Ag^0 species, indicating that the silver deposited on the surface of PMIA fiber was in elemental form.

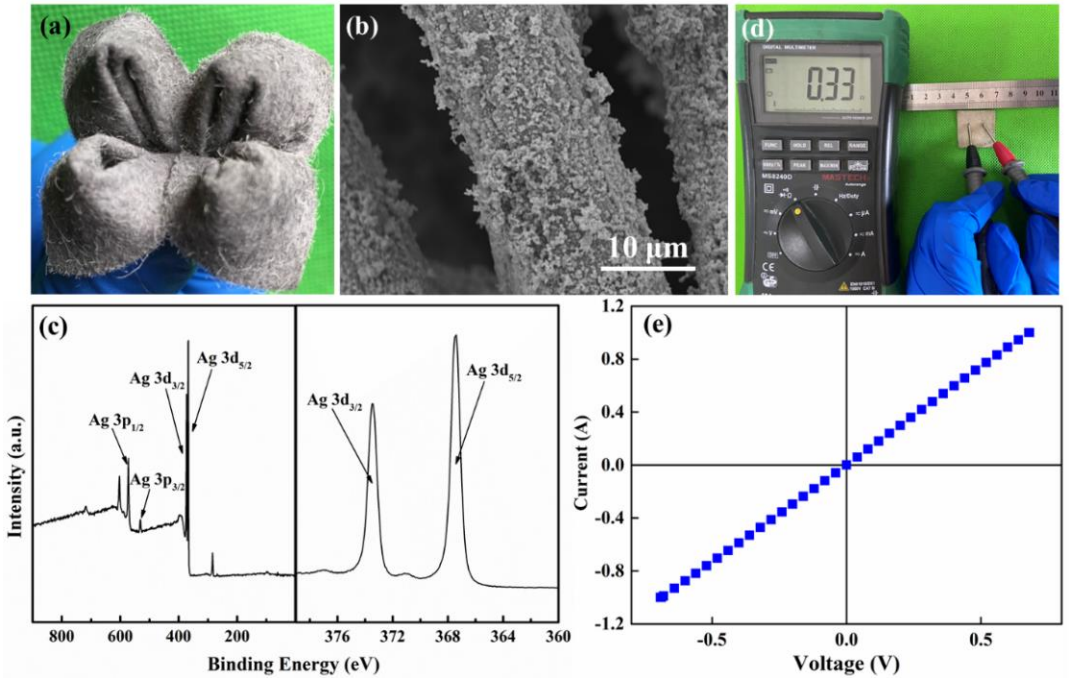

Figure 3. Optical picture (a), SEM image (b), XPS wide scan and Ag 3d spectrum (c), electrical conductivity (d) and *I-V* curve (e) for PMIA/PDA/Ag nonwoven fabric.

As shown in Figure 3d and 3e, silver nanoparticle functionalized PMIA nonwoven fabric showed excellent electrical conductivity with a surface electrical resistance as low as 0.33 Ω over a length of 1 cm (Figure 3d) and a sheet resistance of 0.29 ± 0.026 Ω/sq, respectively. The *I-V* behavior of the PMIA/PDA/Ag nonwoven fabric (4 × 1.5 cm^2) adhered to the Ohs' Law (Figure 3e).

To further demonstrate the electrical performance of the AgNPs functionalized PMIA nonwoven fabric, the silver-coated PMIA nonwoven fabric was connected into an electric circuit with a DC power supply of 3 V. The electrical current of the circuit with only one light bulb (3.8 V/0.3 A) was 0.28 A (Figure S3a, Supporting Information). When the silver-coated PMIA nonwoven fabric (4 × 1.5 cm^2) was connected in series into the circuit, the light bulb

remained well illuminated as shown in Figure S3b (Supporting Information) but the electrical current of the circuit was found to decrease by 7.1% to 0.26 A. This finding reveals the excellent electrical conductivity of the AgNPs functionalized PMIA nonwoven fabric.

In order to determine the effect of PDA modification on the deposition of AgNPs, silver-coated PMIA nonwoven fabric which was not pre-treated with PDA was also prepared. A relatively small amount of AgNPs were deposited on the PMIA fiber surface (Figure S4a and b, Supporting Information), and a conductive layer was not well formed. The light bulb connected with the AgNPs functionalized PMIA nonwoven fabric which was not treated with PDA did not glow up under a DC power supply of 3 V (Figure S4c, Supporting Information). It could be explained by that Ag precursor was not sufficiently absorbed onto fiber surface due to the absence of functional groups on the PMIA. Whereas in contrast, after PDA modification, the catechol and nitrogen-containing groups present in the PDA structure has strong metal-binding ability, resulting in effectively chelation with silver ions and silver nanoparticles reduced in situ [42, 44].

3.3 The effect of silver precursor solution concentration on the morphology and electrical conductivity of silver-coated MAFP nonwoven fabric

SEM images of silver-coated PMIA non-woven fabrics obtained at $AgNO_3$ concentrations ranging from 4 to 12 g/L are shown in Figure 4. It can be clearly seen that at relatively low $AgNO_3$ concentrations of 4 and 6 g/L, the amount of AgNPs was not sufficient to form a continuous coating layer on PMIA fibers (Figure 4a-b). As the $AgNO_3$ concentration increased to 8 g/L and 10 g/L, a relative uniform and continuous layer of AgNPs was found (Figure 4c-d). When the $AgNO_3$ concentration reached 12 g/L, some AgNP agglomerates formed on the PMIA fiber surface due to the excessive silver deposition (Figure 4e).

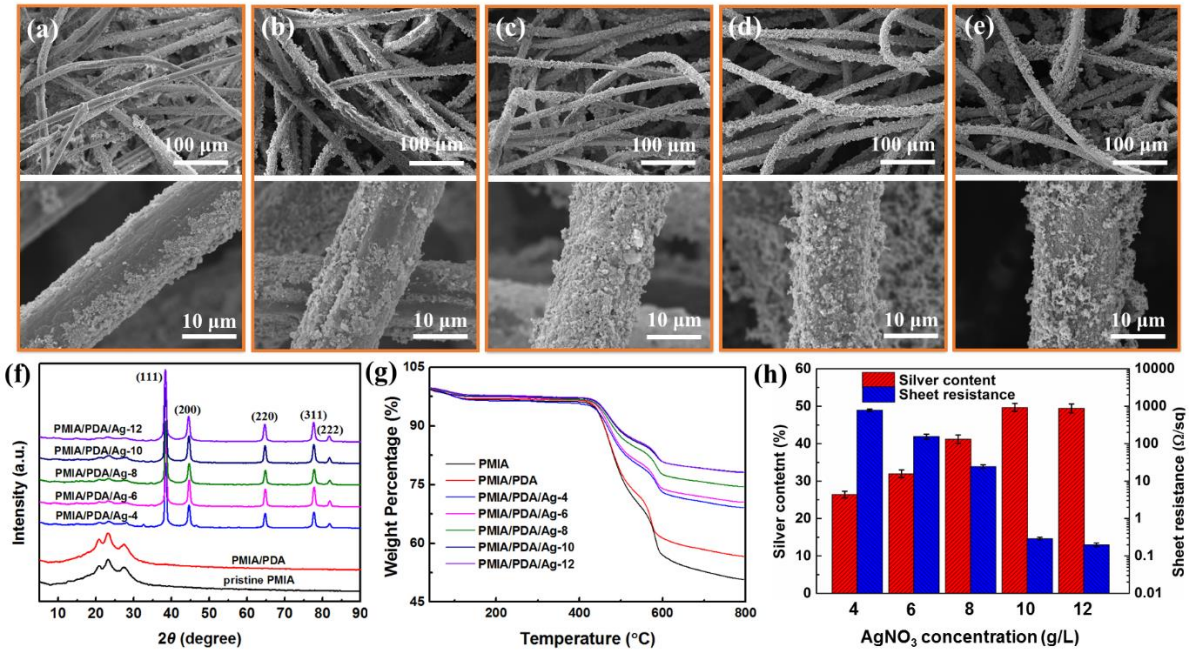

Figure 4. The SEM images of PMIA/PDA/Ag-4 (a), PMIA/PDA/Ag-6 (b), PMIA/PDA/Ag-8 (c), PMIA/PDA/Ag-10 (d), PMIA/PDA/Ag-12 (e) nonwoven fabric; the XRD patterns (f) and thermogravimetric curves (g) of pristine PMIA, dopamine modified PMIA and silver-coated PMIA prepared at different $AgNO_3$ concentrations; the sheet resistance and silver content of PMIA/PDA/Ag nonwoven fabric prepared with different $AgNO_3$ concentration (h).

The formation of AgNPs was confirmed by X-ray diffraction (XRD) pattern, as show in Figure 4f. Obviously, the characteristic peaks of silver-coated PMIA non-woven fabrics were seen at 2θ values of 38.3°, 44.6°, 64.7°, 77.7° and 81.7° corresponding to (111), (200), (220), (311) and (222) planes of face-centered cubic lattice phase silver, respectively. The crystallite size of the silver deposited at different $AgNO_3$ concentration was estimated according to the following equation:

$$D = \frac{k\lambda}{\beta_{1/2}\cos\theta} \qquad (1)$$

where k = 0.89, λ = 0.154 nm, $\beta_{1/2}$ is the full width at half-maximum of the peak for crystal plane, and θ is the diffraction angle. The crystallite size of silver nanoparticles was 13.86, 13.35, 13.09, 13.58 and 13.09 nm for PMIA/PDA/Ag-4, PMIA/PDA/Ag-6, PMIA/PDA/Ag-8

PMIA/PDA/Ag-10 and PMIA/PDA/Ag-12 respectively.

Figure 4g shows the thermogravimetric curves of pristine, PDA modified and silver-coated PMIA nonwoven fabrics obtained at different $AgNO_3$ concentrations. For pristine PMIA nonwoven fabric, there was a weight loss of 3.5% between 30 and 400 °C corresponding to the elimination of water and residual solvent, and then a weight loss of 45.8% between 400 and 800 °C due to partial dehydroxylation and alkoxide decomposition. The initial thermal decomposition temperature of the pristine PMIA nonwoven fabric was 441.9 °C, indicating excellent thermostability. The initial decomposition temperature of PMIA/PDA, PMIA/PDA/Ag-4, PMIA/PDA/Ag-6, PMIA/PDA/Ag-8, PMIA/PDA/Ag-10 and PMIA/PDA/Ag-12 nonwoven fabric was 440.3 °C, 441.6 °C, 441.2 °C, 442.0 °C, 440.2 °C and 440.8 °C respectively, revealing that the high thermal stability of PMIA nonwoven fabric was well maintained after PDA modification and AgNPs functionalization. The silver content was calculated from the thermogravimetric data according to the following equation:

$$w_{Ag} = \frac{w_a - w_b}{1 - w_b} \qquad (2)$$

where w_a and w_b is the residual mass fraction of silver-coated PMIA and PDA modified PMIA respectively. Figure 4h shows that the content of AgNPs in silver-coated PMIA nonwoven fabric increased with increasing $AgNO_3$ concentration and the electrical sheet resistance decreased accordingly. When the $AgNO_3$ concentration was 10 g/L, the silver content reached 49.67% and the sheet resistance was as low as 0.29 ± 0.026 Ω/sq, which outperformed previously reported conductive fabrics [23, 45-47]. The significant increase in electrical conductivity with increasing $AgNO_3$ concentration was mainly attributed to the formation of highly conductive AgNP networks. There was no significant change in the electrical conductivity when the $AgNO_3$ concentration was increased further to 12 g/L (0.2 ± 0.022 Ω/sq), indicating that the concentration of 10 g/L was sufficient to form continuous AgNP networks on PMIA nonwoven fabrics. The above results indicate that the $AgNO_3$ precursor concentration

had a great influence on the amount of AgNPs deposited on the PMIA nonwoven fabric surface and the electrical conductivity of the AgNPs functionalized PMIA nonwoven fabric, but did not introduce significant effect on the crystallite size of AgNPs.

The EMI shielding effectiveness in X-band (8.2-12.4 GHz) of silver-coated PMIA non-woven fabric prepared with different $AgNO_3$ concentrations was evaluated. Figure 5a shows that pristine PMIA non-woven fabric does not have EMI shielding effectiveness. Silver-coated PMIA non-woven fabric prepared at $AgNO_3$ concentration of 4, 6 and 8 g/L had the value of EMI SE of 1.38 dB, 2.05 dB and 5.54 dB respectively, which were far lower than the requirement for commercial EMI shielding materials (30 dB). When the $AgNO_3$ concentration was increased to 10 g/L, the EMI SE of silver-coated PMIA non-woven fabric reached a mean value of 92.6 dB over 8.2-12.4 GHz, which was higher than those of previously reported AgNPs or AgNWs functionalized composite EMI shielding materials [10, 12, 23, 48, 49]. The increased electrical conductivity was responsible for increased EMI SE for silver-coated PMIA nonwoven fabric. When the $AgNO_3$ concentration increased further to 12 g/L, the EMI SE increased to 110.9 dB.

It is well known that the density and thickness of the shielding material have great influence on the EMI shielding performance. Thus, in the present study the specific EMI shielding effectiveness (SSE, EMI SE divided by the density of the sample) and the absolute EMI shielding effectiveness (SSE/t, SSE divided by the thickness of the material) were further introduced to evaluate the EMI shielding performance. The EMI shielding material reported in the literatures are summarized in Fig. 5b, it can be found that the PMIAPDA/Ag-10 possessed high SSE of 245.8 dB cm^3/g and SSE/t of 8194.7 dB cm^2/g (the area density of PMIAPDA/Ag-10 was approximated to be 113 g/m^2, which was determined based on the content of PDA and AgNPs in PMIA nonwoven fabric from TG test). These results highlight that the AgNPs functionalized PMIA nonwoven fabrics are promising candidates for EMI shielding

applications.

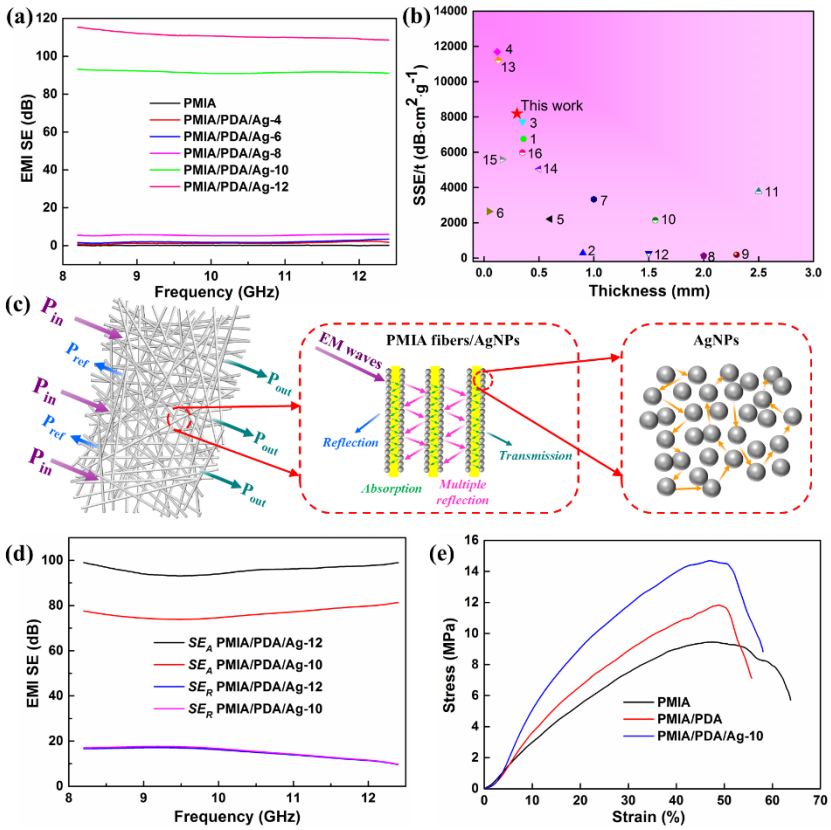

Figure 5. The EMI shielding effectiveness of pristine PMIA and silver-coated PMIA prepared at different $AgNO_3$ concentrations (a); comparison of the EMI shielding performance of various materials (b); the shielding mechanism of the AgNPs functionalized PMIA nonwoven fabric (c); the SE_A and SE_R of PMIA/PDA/Ag-10 and PMIA/PDA/Ag-12 (d); The stress-strain curves of pristine PMIA, PMIA/PDA and PMIA/PDA/Ag-10 nonwoven fabrics (e).

The outstanding EMI shielding performance of the AgNPs functionalized PMIA could be attributed to the high electrical conductivity and the continuity of the fibrous structures of the silver-coated PMIA nonwoven fabric. A shielding mechanism has been proposed to understand the EMI shielding performance of silver-coated PMIA nonwoven fabric, as shown in Figure 5c. When the EM waves reached the silver-coated PMIA nonwoven fabric, some of EM waves could be reflected directly on the surface due to the abundant free electrons at the surface of AgNPs [50]. Then, the remaining EM waves would enter the nonwoven fabric, where they strike the high-electron density of AgNPs inside the silver-coated PMIA nonwoven fabric, the

induced currents would produce ohmic losses [10, 11] and weaken the EM wave energy. As the silver-coated PMIA nonwoven fabric had a porous structure present in interfiber spaces, the EM waves could be reflected back and forth among the large amount of interfacial areas and be effectively attenuated inside the porous nonwoven structure before they were emitted [10, 51]. Furthermore, after AgNPs deposition, the surface of PMIA fibers became rough with many voids, which could also efficiently attenuate EM waves through multiple internal reflections and then absorptions [36].

Generally, the total EMI SE (SE_{Total}) is the sum of the effectiveness of absorption loss (SE_A), reflection loss (SE_R) and multiple reflection (SE_M). SE_M is generally negligible when the value of SE_{Total} is above 15 dB [52]. The reflection loss is determined by an impedance mismatch between air and the shielding material, while the absorption loss is determined by both the conductivity and the thickness of shielding materials [11]. As shown in Figure 5d, SE_A was much higher than SE_R over the frequency range of 8.2-12.4 GHz for both PMIA/PDA/Ag-10 and PMIA/PDA/Ag-12 nonwoven fabrics. The power coefficient of reflectance (R) and absorbance (A) and transmittance (T) was used for analyzing the shielding mechanism [10]. The R and A for PMIA/PDA/Ag-10 was 94.3% and 5.7% respectively, indicating the reflection dominant shielding mechanism.

Skin depth (δ) is an important parameter in determining the shielding capability. δ is defined as the depth where the amplitude of EM waves decreases to $1/e$ of its original value and can be calculated by using the equation (3) [53].

$$\delta = \sqrt{\frac{1}{\pi f \mu \sigma}} \quad \text{when } \sigma >> 2\pi f \varepsilon_0,\ \mu = \mu_0 \mu_r \qquad (3)$$

where f is the frequency, σ is the electrical conductivity, μ represents the magnetic permeability of the material and ε_0 is the vacuum permittivity. As the silver-coated PMIA nonwoven fabric is nonmagnetic, $\mu_0 = 4\pi \times 10^{-7}$ Hm^{-1} and $\mu_r = 1$ [54].

For PMIA/PDA/Ag-10 nonwoven fabric, the calculated δ value at 8.2 GHz and 12.4 GHz was

0.052 mm and 0.042 mm respectively, which is thinner than the thickness of the tested sample (0.3 mm). The theoretical EMI shielding performance of the PMIA/PDA/Ag-10 nonwoven fabric was calculated using the following equations [48]:

$$SE_A = 8.7d\sqrt{\pi f \mu \sigma} = 8.7\frac{d}{\delta} \quad (4)$$

$$SE_R = 39.5 + 10log\frac{\sigma}{2\pi f \mu} \quad (5)$$

Where *d* is the sample thickness.

The theoretical value of SE_R, SE_A and SE_{Total} at 12.4 GHz was 30.03 dB, 61.7 dB and 91.73 dB, respectively, which was in good agreement with the experimental value. Compared with the theoretical analysis results, the experimental value of *R* was lower while the experimental value of *A* was higher. It could be explained that the large surface and interface areas in the porous silver-coated PMIA nonwoven fabric can effectively prevent electromagnetic waves from passing through the fabrics via reflection and scattering, which causes electromagnetic waves to be absorbed or dissipated as heat [25].

Besides high EMI shielding effectiveness, appropriate mechanical performance is also crucial for practical engineering application of EMI shielding materials under extreme conditions. Figure 5e shows the typical stress-strain curves which were plotted based on the tensile tests of pristine PMIA, PMIA/PDA and PMIA/PDA/Ag-10 nonwoven fabrics. It can be noted that the introduction of PDA coating and/or AgNPs improved mechanical properties of PMIA nonwoven fabrics in terms of tensile strength and Young's modulus. For example, the tensile strength and Young's modulus of AgNPs functionalized PMIA nonwoven fabric was 14.81 ± 0.59 MPa and 61.34 ± 4.82 MPa respectively, which was 55.6% and 78.8% higher than those of pristine PMIA nonwoven fabric.

3.4 Washing and bending fastness of silver-coated PMIA non-woven fabric

The stability of EMI shieling effectiveness under washing and mechanical deformation is a decisive factor enabling the practical application of shielding materials in flexible and wearable

electronic devices. Herein, the coating durability of the PMIA/PDA/Ag-10 nonwoven fabric subjected to washing and mechanical bending and torsion was evaluated. The washing fastness of silver-plated PMIA non-woven fabrics was tested on a textile-color fastness meter (SW-20B, Quanzhou MeiBang Instrument Co., Ltd). Specifically, a piece of PMIA/PDA/Ag-10 nonwoven fabric (4 × 1.5 cm^2) was placed in a sample cup containing a standard water bath of 50 ml. Silver-plated PMIA non-woven fabric samples were washed for five cycles and for a single washing cycle the washing condition was set at 40 °C for 30 min with the sample cup rotating at 40 rpm. After washing three times with distilled water, silver-plated PMIA non-woven fabric samples were dried in a vacuum oven at 60 °C overnight and used for further testing. As shown in Figure 6a, the value of sheet resistance of the PMIA/PDA/Ag-10 nonwoven fabric increased from 0.29 ± 0.026 Ω/sq to 0.34 ± 0.03 Ω/sq after 5 washing cycles. The corresponding SEM observation after washing shown in Figure 6b revealed that the AgNP networks were well preserved with only some small amount peeling-off of the silver coating on the fiber surface.

Figure 6c shows that PMIA/PDA/Ag-10 nonwoven fabric (4 × 1.5 cm^2) presented small changes in electrical resistance subject to bending or torsion, with a maximum $\Delta R/R_0$ of 0.16 occurring to a torsion of 540°. Furthermore, the long-term stability of the PMIA/PDA/Ag-10 nonwoven fabric (4 × 1.5 cm^2) was also evaluated by performing cyclic bending/releasing testing under a chord length of 20 mm (Figure 6d). The gradual change in electrical resistance might be attributed to the fracture of the weak and fragile conductive AgNP pathways upon bending deformation [21]. A relatively small increase in the resistance from 0.65 Ω to 0.73 Ω was observed after bending 1000 cycles. The reliable electrical conductivity during the bending deformation was due to the well-preserved conductive AgNP networks, although small cracks appeared on some individual fiber (Figure 6e).

As shown in Figure 6f, the EMI SE of PMIA/PDA/Ag-10 nonwoven fabric decreased slightly

from 92.6 dB to 89 dB after 5 washing cycles and to 84.5 dB after 1000 bending cycles. These results indicate the AgNPs functionalized PMIA nonwoven fabric had good long-term structural and performance stability and could act as a promising flexible EMI shielding material candidate.

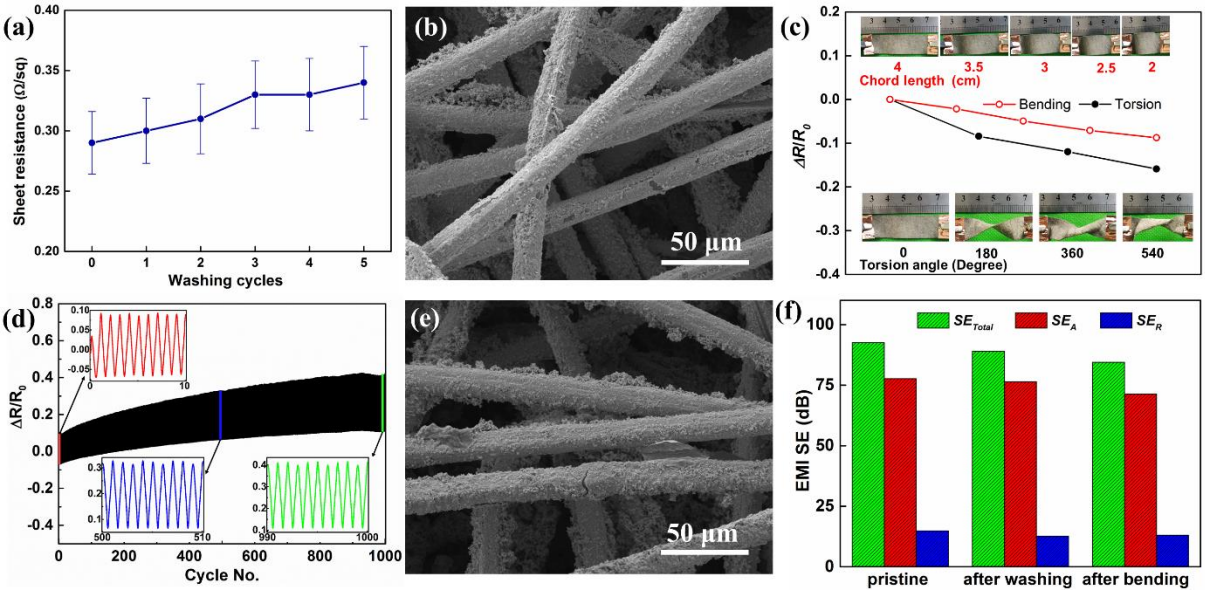

Figure 6. The relationship between sheet resistance with washing cycles (a); the SEM image after 5 washing cycles (b); the relative electrical resistance change during bending and torsion tests (c); the relative electrical resistance change during 1000 cycles of bending tests (d); the SEM image after 1000 bending/releasing cycles (e) and the EMI SE after 5 washing cycles and 1000 bending cycles for PMIA/PDA/Ag-10 nonwoven fabric (f).

3.5 Temperature and chemical stability of silver-coated PMIA nonwoven fabric

To further demonstrate the performance of AgNPs functionalized PMIA nonwoven fabric, the electrical conductivity and EMI shielding performance of silver-coated PMIA nonwoven fabric were evaluated under conditions of high/low temperature, acid/alkali solutions and various organic solvents. Figure 7a shows the change of electrical resistance of PMIA/PDA/Ag-10 nonwoven fabric in the temperature range of -80 – 200 °C. The sheet resistance was measured after the sample was placed under the corresponding temperature for 2 h. The result showed that when the temperature changed between -80 to 200 °C, the sheet resistance slightly varied

between 0.28 Ω/sq and 0.33 Ω/sq, indicating that silver-coated PMIA nonwoven fabric can maintain excellent electrical conductivity in a wide temperature range.

To demonstrate the chemical stability of silver-coated PMIA nonwoven fabric, samples with 55 mm in length and 15 mm in width was firstly immersed in hydrochloric acid with a pH value of 2.0, sodium hydroxide with a pH value of 12.0 and various organic solvents (N-heptane, acetone, ethanol, xylene and DMF) for 7 days. Then the sheet resistance and EMI SE performance of the samples were measured after being dried. As can be seen from Figure 7b, the PMIA/PDA/Ag-10 nonwoven fabric maintained excellent electrical conductivity after being soaked in the acid/alkali solutions and the above-mentioned organic solvents. The sheet resistance of the sample after acid/alkali and organic solvents treatment was below 0.39 Ω/sq except for the DMF treated sample, whose sheet resistance increased to 0.54 Ω/sq. The more remarkable increase in sheet resistance for DMF treated sample might be due to the destruction of PMIA nonwoven fabric by DMF. The solutions in the bottle remained clear and transparent after the silver-coated PMIA nonwoven fabric were immersed for 7 days, as shown in the inserted image of Figure 7b. The above results verified the chemical stability of AgNPs functionalized PMIA nonwoven fabric. Figure 7c shows that the EMI SE of silver-coated PMIA nonwoven fabric after being exposed to high/low temperature, acid/alkali solutions and various organic solvents was above 65 dB, which was far above the requirement for commercial EMI shielding materials of 30 dB.

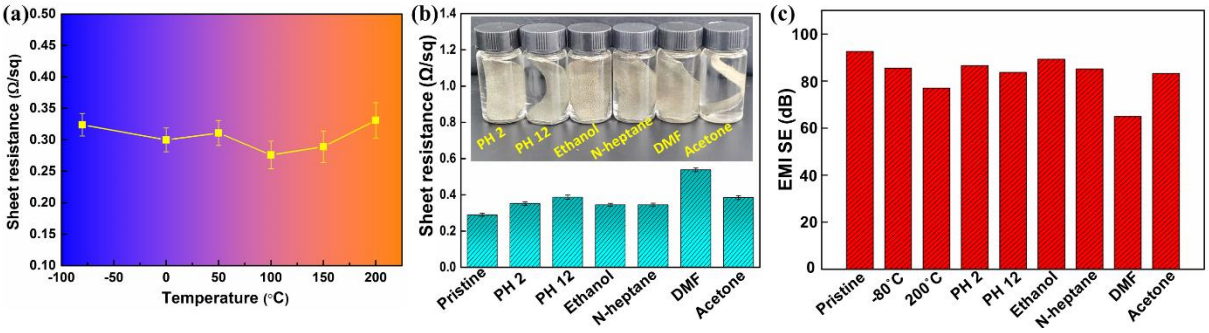

Figure 7. The variation of sheet resistance for PMIA/PDA/Ag-10 nonwoven fabric after being

treated for 2 h at different temperature (a) and after being immersed 7 days in acid/alkali solution and various organic solvents (b); The EMI SE of pristine silver-coated PMIA and silver-coated PMIA treated at different temperature for 2 h and immersed in acid/alkali solution and various organic solvents for 7 days (c).

4. Conclusions

AgNPs functionalized PMIA non-woven fabric with high electrical conductivity and excellent electromagnetic shielding efficiency was fabricated by combining polydopamine modification and electroless silver plating. The presence of polydopamine greatly enhanced the efficient deposition of AgNPs and the interfacial cohesion between the AgNPs and the PMIA fibers. The silver-coated PMIA non-woven fabric thus prepared exhibited a high electrical conductivity of 0.29 Ω/sq, an excellent EMI SE of 92.6 dB and a high absolute EMI SE of 8194.7 $dB \cdot cm^2 \cdot g^{-1}$ (when the $AgNO_3$ concentration was 10 g/L). In addition, the silver-coated PMIA non-woven fabric presented high resistance to washing, bending and torsion deformations, high/low temperature, strong acidic/alkaline solutions and different organic solvents, as reflected by the retention of high electrical conductivity and EMI SE. The findings of this work provide a novel methodology into the preparation of high-performance flexible electromagnetic shielding materials that have the capability to be used in various harsh conditions.

Acknowledgements

The authors would like to thank the financial support from the Shandong Provincial Key Research and Development Program, China (Grant no. 2019GGX102071), the National Natural Science Foundation of China (Grant no. 51703108) and the Shandong "Taishan Youth Scholar Program" (Grant no. tsqn201909100).

Supporting information

FTIR of PMIA nonwoven fabric; Water contact angle of pristine PMIA nonwoven fabric; The electrical conductivity of PMIA nonwoven fabric; Surface morphology and electrical

conductivity of silver-coated PMIA nonwoven fabric without PDA modification; Comparison of the EMI SE of different materials.

Movie S1 showing the water contact angle test of PMIA/PDA nonwoven fabric.

Ethics declarations

Conflict of Interest: The authors declare that they have no conflict of interest.

References

[1] H. Aniołczyk, EM Noise and Its Impact on Human Health and Safety, Advanced Materials for Electromagnetic Shielding, (2018) 11-33.
[2] Y.J. Tan, J. Li, J.H. Cai, X.H. Tang, J.H. Liu, Z.Q. Hu, M. Wang, Comparative study on solid and hollow glass microspheres for enhanced electromagnetic interference shielding in polydimethylsiloxane/multi-walled carbon nanotube composites, Composites Part B: Engineering, 177 (2019) 107378.
[3] Y. Bhattacharjee, I. Arief, S. Bose, Recent trends in multi-layered architectures towards screening electromagnetic radiation: challenges and perspectives, Journal of Materials Chemistry C, 5 (2017) 7390-7403.
[4] G.M. Weng, J.Y. Li, M. Alhabeb, C. Karpovich, H. Wang, J. Lipton, K. Maleski, J. Kong, E. Shaulsky, M. Elimelech, Y. Gogotsi, A.D. Taylor, Layer-by-Layer Assembly of Cross-Functional Semi-transparent MXene-Carbon Nanotubes Composite Films for Next-Generation Electromagnetic Interference Shielding, Advanced Functional Materials, 28 (2018) 1803360.
[5] J. Lee, Y. Liu, Y. Liu, S.J. Park, M. Park, H.Y. Kim, Ultrahigh electromagnetic interference shielding performance of lightweight, flexible, and highly conductive copper-clad carbon fiber nonwoven fabrics, Journal of Materials Chemistry C, 5 (2017) 7853-7861.
[6] P. Sambyal, A. Iqbal, J. Hong, H. Kim, M.K. Kim, S.M. Hong, M. Han, Y. Gogotsi, C.M. Koo, Ultralight and Mechanically Robust Ti3C2Tx Hybrid Aerogel Reinforced by Carbon Nanotubes for Electromagnetic Interference Shielding, ACS Applied Materials & Interfaces, (2019).
[7] K.S. Dijith, R. Aiswarya, M. Praveen, S. Pillai, K.P. Surendran, Polyol derived Ni and NiFe alloys for effective shielding of electromagnetic interference, Materials Chemistry Frontiers, 2 (2018) 1829-1841.
[8] F. Kargar, Z. Barani, M. Balinskiy, A.S. Magana, J.S. Lewis, A.A. Balandin, Dual-Functional Graphene Composites for Electromagnetic Shielding and Thermal Management, Advanced Electronic Materials, 5 (2019) 1800558.
[9] Y.D. Shi, J. Li, Y.J. Tan, Y.F. Chen, M. Wang, Percolation behavior of electromagnetic interference shielding in polymer/multi-walled carbon nanotube nanocomposites, Composites Science and Technology, 170 (2019) 70-76.
[10] J. Gao, J. Luo, L. Wang, X. Huang, H. Wang, X. Song, M. Hu, L.C. Tang, H. Xue, Flexible, superhydrophobic and highly conductive composite based on non-woven polypropylene fabric for electromagnetic interference shielding, Chemical Engineering Journal, 364 (2019) 493-502.
[11] H. Ji, R. Zhao, N. Zhang, C. Jin, X. Lu, C. Wang, Lightweight and flexible electrospun polymer nanofiber/metal nanoparticle hybrid membrane for high-performance electromagnetic

interference shielding, NPG Asia Materials, 10 (2018) 749-760.
[12] T.W. Lee, S.E. Lee, Y.G. Jeong, Highly Effective Electromagnetic Interference Shielding Materials based on Silver Nanowire/Cellulose Papers, ACS Applied Materials & Interfaces, 8 (2016) 13123-13132.
[13] C. Liu, J. Liu, X. Ning, S. Chen, Z. Liu, S. Jiang, D. Miao, The Effect of Polydopamine on an Ag-Coated Polypropylene Nonwoven Fabric, Polymers, 11 (2019) 627.
[14] X. Yang, S. Fan, Y. Li, Y. Guo, Y. Li, K. Ruan, S. Zhang, J. Zhang, J. Kong, J. Gu, Synchronously improved electromagnetic interference shielding and thermal conductivity for epoxy nanocomposites by constructing 3D copper nanowires/thermally annealed graphene aerogel framework, Composites Part A: Applied Science and Manufacturing, 128 (2020) 105670.
[15] H. Nallabothula, Y. Bhattacharjee, L. Samantara, S. Bose, Processing-Mediated Different States of Dispersion of Multiwalled Carbon Nanotubes in PDMS Nanocomposites Influence EMI Shielding Performance, ACS Omega, 4 (2019) 1781-1790.
[16] Y. Wang, W. Li, Y. Zhou, L. Jiang, J. Ma, S. Chen, S. Jerrams, F. Zhou, Fabrication of high-performance wearable strain sensors by using CNTs-coated electrospun polyurethane nanofibers, J. Mater. Sci., 55 (2020) 12592-12606.
[17] J. Li, J.L. Chen, X.H. Tang, J.H. Cai, J.H. Liu, M. Wang, Constructing nanopores in poly(oxymethylene)/multi-wall carbon nanotube nanocomposites via poly(l-lactide) assisting for improving electromagnetic interference shielding, Journal of Colloid and Interface Science, 565 (2020) 536-545.
[18] Y. Yuan, W. Yin, M. Yang, F. Xu, X. Zhao, J. Li, Q. Peng, X. He, S. Du, Y. Li, Lightweight, flexible and strong core-shell non-woven fabrics covered by reduced graphene oxide for high-performance electromagnetic interference shielding, Carbon, 130 (2018) 59-68.
[19] W. Li, Y. Zhou, Y. Wang, Y. Li, L. Jiang, J. Ma, S. Chen, Highly Stretchable and Sensitive SBS/Graphene Composite Fiber for Strain Sensors, Macromolecular Materials and Engineering, 305 (2020) 1900736.
[20] C. Liang, P. Song, H. Qiu, Y. Zhang, X. Ma, F. Qi, H. Gu, J. Kong, D. Cao, J. Gu, Constructing interconnected spherical hollow conductive networks in silver platelets/reduced graphene oxide foam/epoxy nanocomposites for superior electromagnetic interference shielding effectiveness, Nanoscale, 11 (2019) 22590-22598.
[21] Q.W. Wang, H.B. Zhang, J. Liu, S. Zhao, X. Xie, L. Liu, R. Yang, N. Koratkar, Z.Z. Yu, Multifunctional and Water-Resistant MXene-Decorated Polyester Textiles with Outstanding Electromagnetic Interference Shielding and Joule Heating Performances, Advanced Functional Materials, 29 (2019) 1806819.
[22] Y. Zhang, L. Wang, J. Zhang, P. Song, Z. Xiao, C. Liang, H. Qiu, J. Kong, J. Gu, Fabrication and investigation on the ultra-thin and flexible Ti3C2Tx/co-doped polyaniline electromagnetic interference shielding composite films, Composites Science and Technology, 183 (2019) 107833.
[23] L.X. Liu, W. Chen, H.B. Zhang, Q.W. Wang, F.L. Guan, Z.Z. Yu, Flexible and Multifunctional Silk Textiles with Biomimetic Leaf-Like MXene/Silver Nanowire Nanostructures for Electromagnetic Interference Shielding, Humidity Monitoring, and Self-Derived Hydrophobicity, Advanced Functional Materials, 29 (2019) 1905197.
[24] R. Kumaran, S.D. kumar, N. Balasubramanian, M. Alagar, V. Subramanian, K. Dinakaran,

Enhanced Electromagnetic Interference Shielding in a Au–MWCNT Composite Nanostructure Dispersed PVDF Thin Films, The Journal of Physical Chemistry C, 120 (2016) 13771-13778.
[25] L.C. Jia, L. Xu, F. Ren, P.G. Ren, D.X. Yan, Z.M. Li, Stretchable and durable conductive fabric for ultrahigh performance electromagnetic interference shielding, Carbon, 144 (2019) 101-108.
[26] L. Wang, H. Qiu, C. Liang, P. Song, Y. Han, Y. Han, J. Gu, J. Kong, D. Pan, Z. Guo, Electromagnetic interference shielding MWCNT-Fe3O4@Ag/epoxy nanocomposites with satisfactory thermal conductivity and high thermal stability, Carbon, 141 (2019) 506-514.
[27] Y. Gao, X. Gao, J. Li, S. Guo, Improved microwave absorbing property provided by the filler's alternating lamellar distribution of carbon nanotube/ carbonyl iron/ poly (vinyl chloride) composites, Composites Science and Technology, 158 (2018) 175-185.
[28] S. Biswas, S.S. Panja, S. Bose, Tailored distribution of nanoparticles in bi-phasic polymeric blends as emerging materials for suppressing electromagnetic radiation: challenges and prospects, Journal of Materials Chemistry C, 6 (2018) 3120-3142.
[29] S. Li, J. Li, N. Ma, D. Liu, G. Sui, Super-Compression-Resistant Multiwalled Carbon Nanotube/Nickel-Coated Carbonized Loofah Fiber/Polyether Ether Ketone Composite with Excellent Electromagnetic Shielding Performance, ACS Sustainable Chemistry & Engineering, 7 (2019) 13970-13980.
[30] L. Wu, L. Wang, Z. Guo, J. Luo, H. Xue, J. Gao, Durable and Multifunctional Superhydrophobic Coatings with Excellent Joule Heating and Electromagnetic Interference Shielding Performance for Flexible Sensing Electronics, ACS Applied Materials & Interfaces, 11 (2019) 34338-34347.
[31] Y. Zhou, Z. Sun, L. Jiang, S. Chen, J. Ma, F. Zhou, Flexible and conductive meta-aramid fiber paper with high thermal and chemical stability for electromagnetic interference shielding, Applied Surface Science, 533 (2020) 147431.
[32] K. Zhang, H.-O. Yu, K.-X. Yu, Y. Gao, M. Wang, J. Li, S. Guo, A facile approach to constructing efficiently segregated conductive networks in poly(lactic acid)/silver nanocomposites via silver plating on microfibers for electromagnetic interference shielding, Composites Science and Technology, 156 (2018) 136-143.
[33] L. Xu, X.P. Zhang, C.H. Cui, P.G. Ren, D.X. Yan, Z.M. Li, Enhanced Mechanical Performance of Segregated Carbon Nanotube/Poly(lactic acid) Composite for Efficient Electromagnetic Interference Shielding, Industrial & Engineering Chemistry Research, 58 (2019) 4454-4461.
[34] Z. Zeng, M. Chen, Y. Pei, S.I. Seyed Shahabadi, B. Che, P. Wang, X. Lu, Ultralight and Flexible Polyurethane/Silver Nanowire Nanocomposites with Unidirectional Pores for Highly Effective Electromagnetic Shielding, ACS Applied Materials & Interfaces, 9 (2017) 32211-32219.
[35] X. Fan, G. Zhang, Q. Gao, J. Li, Z. Shang, H. Zhang, Y. Zhang, X. Shi, J. Qin, Highly expansive, thermally insulating epoxy/Ag nanosheet composite foam for electromagnetic interference shielding, Chemical Engineering Journal, 372 (2019) 191-202.
[36] Y.J. Tan, J. Li, Y. Gao, J. Li, S.Y. Guo, M. Wang, A facile approach to fabricating silver-coated cotton fiber non-woven fabrics for ultrahigh electromagnetic interference shielding, Applied Surface Science, 458 (2018) 236-244.
[37] Z. Wang, T. Li, J. Yu, Z. Hu, J. Zhu, Y. Wang, General Bioinspired, Innovative Method for

Fabrication of Surface-Nickeled Meta-aramid Fibers, Industrial & Engineering Chemistry Research, 58 (2019) 9458-9464.
[38] S.Y. Ryu, J.W. Chung, S.Y. Kwak, Amphiphobic meta-aramid nanofiber mat with improved chemical stability and mechanical properties, European Polymer Journal, 91 (2017) 111-120.
[39] J. Jung, H. Lee, I. Ha, H. Cho, K.K. Kim, J. Kwon, P. Won, S. Hong, S.H. Ko, Highly Stretchable and Transparent Electromagnetic Interference Shielding Film Based on Silver Nanowire Percolation Network for Wearable Electronics Applications, ACS Applied Materials & Interfaces, 9 (2017) 44609-44616.
[40] H. Lee, S.M. Dellatore, W.M. Miller, P.B. Messersmith, Mussel-Inspired Surface Chemistry for Multifunctional Coatings, Science, 318 (2007) 426-430.
[41] Y. Zhou, L. Li, W. Li, S. Wen, L. Jiang, S. Jerrams, J. Ma, S. Chen, The Fabrication and properties of magnetorheological elastomers employing bio-inspired dopamine modified carbonyl iron particles, Smart Mater. Struct., 29 (2020) 055005.
[42] W. Wang, R. Li, M. Tian, L. Liu, H. Zou, X. Zhao, L. Zhang, Surface Silverized Meta-Aramid Fibers Prepared by Bio-inspired Poly(dopamine) Functionalization, ACS Applied Materials & Interfaces, 5 (2013) 2062-2069.
[43] Y. Fu, L. Liu, L. Zhang, W. Wang, Highly Conductive One-Dimensional Nanofibers: Silvered Electrospun Silica Nanofibers via Poly(dopamine) Functionalization, ACS Applied Materials & Interfaces, 6 (2014) 5105-5112.
[44] W. Hu, Z. Zeng, Z. Wang, C. Liu, X. Wu, Q. Gu, Facile fabrication of conductive ultrahigh molecular weight polyethylene fibers via mussel-inspired deposition, Journal of Applied Polymer Science, 128 (2013) 1030-1035.
[45] S.K. Sinha, F.A. Alamer, S.J. Woltornist, Y. Noh, F. Chen, A. McDannald, C. Allen, R. Daniels, A. Deshmukh, M. Jain, K. Chon, D.H. Adamson, G.A. Sotzing, Graphene and Poly(3,4-ethylene dioxythiophene):Poly(4-styrenesulfonate) on Nonwoven Fabric as a Room Temperature Metal and Its Application as Dry Electrodes for Electrocardiography, ACS Applied Materials & Interfaces, 11 (2019) 32339-32345.
[46] M.S. Sadi, J.J. Pan, A.C. Xu, D.S. Cheng, G.M. Cai, X. Wang, Direct dip-coating of carbon nanotubes onto polydopamine-templated cotton fabrics for wearable applications, Cellulose, 26 (2019) 7569-7579.
[47] Z.L. Liu, Z. Li, L. Cheng, S.H. Chen, D.Y. Wu, F.Y. Dai, Reduced Graphene Oxide Coated Silk Fabrics with Conductive Property for Wearable Electronic Textiles Application, Advanced Electronic Materials, 5 (2019) 9.
[48] J. Luo, L. Wang, X. Huang, B. Li, Z. Guo, X. Song, L. Lin, L. Tang, H. Xue, J. Gao, Mechanically Durable, Highly Conductive, and Anticorrosive Composite Fabrics with Excellent Self-Cleaning Performance for High-Efficiency Electromagnetic Interference Shielding, ACS Applied Materials & Interfaces, 11 (2019) 10883-10894.
[49] L.C. Jia, G.Q. Zhang, L. Xu, W.J. Sun, G.J. Zhong, J. Lei, D.X. Yan, Z.M. Li, Robustly Superhydrophobic Conductive Textile for Efficient Electromagnetic Interference Shielding, ACS Applied Materials & Interfaces, 11 (2019) 1680-1688.
[50] F. Shahzad, M. Alhabeb, C.B. Hatter, B. Anasori, S. Man Hong, C.M. Koo, Y. Gogotsi, Electromagnetic interference shielding with 2D transition metal carbides (MXenes), Science, 353 (2016) 1137-1140.

[51] T.T. Li, Y. Wang, H.K. Peng, X. Zhang, B.C. Shiu, J.H. Lin, C.W. Lou, Lightweight, flexible and superhydrophobic composite nanofiber films inspired by nacre for highly electromagnetic interference shielding, Composites Part A: Applied Science and Manufacturing, 128 (2020) 105685.
[52] Z. Chen, C. Xu, C. Ma, W. Ren, H.M. Cheng, Lightweight and Flexible Graphene Foam Composites for High-Performance Electromagnetic Interference Shielding, 25 (2013) 1296-1300.
[53] A.K. Singh, A. Shishkin, T. Koppel, N. Gupta, A review of porous lightweight composite materials for electromagnetic interference shielding, Composites Part B: Engineering, 149 (2018) 188-197.
[54] Y.J. Wan, P.L. Zhu, S.H. Yu, R. Sun, C.P. Wong, W.H. Liao, Anticorrosive, Ultralight, and Flexible Carbon-Wrapped Metallic Nanowire Hybrid Sponges for Highly Efficient Electromagnetic Interference Shielding, Small, 14 (2018) 1800534.

Graphical Abstract